

1 The in vivo assessment of thoracic vertebral shape from MRI data using  
2 a shape model

3

4

5

## 6 **Structured Abstract**

### 7 **Study design**

8 Feasibility study on characterising thoracic vertebral shape from magnetic resonance images  
9 using a shape model.

### 10 **Objectives**

11 Assess the reliability of characterising thoracic vertebral shape from magnetic resonance  
12 images and estimate the normal variation in vertebral shape using a shape model.

### 13 **Summary of background data**

14 The characterisation of thoracic vertebrae shape is important for understanding the initiation  
15 and progression of deformity and in developing surgical methods. Methods for characterising  
16 shape need to be comprehensive, reliable and suitable for use in vivo.

### 17 **Methods**

18 Magnetic resonance images of the thoracic vertebrae were acquired from 20 adults. Repeat  
19 scans were acquired, after repositioning the participants, for T4, T8 and T12. Landmark points  
20 were placed around the vertebra on the images and used to create a shape model. The  
21 reliability was assessed using relative error (E%) and intra-class correlation (ICC). The effect of  
22 vertebral level, sex and age on vertebral shape was assessed using repeated measures analysis  
23 of variance.

### 24 **Results**

25 Five modes of variation were retained from the shape model. Reliability was excellent for the  
26 first two modes (mode 1: E% = 7, ICC = 0.98; mode 2: E% = 11, ICC = 0.96). These modes

27 described variation in the vertebral bodies, the pedicle width and orientation, and the facet  
28 joint position and orientation with respect to the pedicle axis. Variation in vertebral shape was  
29 found along the thoracic spine and between individuals, but there was little effect of age and  
30 sex.

### 31 **Conclusions**

32 Magnetic resonance images and shape modelling provides a reliable method for characterising  
33 vertebral shape in vivo. The method is able to identify differences between vertebral levels and  
34 between individuals. The use of these methods may be advantageous for performing repeated  
35 measurements in longitudinal studies.

### 36 **Level of Evidence**

37 N/A

38

39

40 **Key Words**

41 Thoracic vertebrae

42 Magnetic resonance imaging

43 Statistical shape model

44 Reliability of results

45 Anatomy

46

47

## 48 **Introduction**

49 The characterisation of thoracic vertebral shape is important for helping us understand the  
50 aetiology and pathogenesis of spinal deformity and for developing optimal treatments. Many  
51 previous studies have characterised the shape of the thoracic vertebrae and shown it to exhibit  
52 considerable variation within the normal population and in the presence of pathology such as  
53 scoliosis [1] but these studies have mostly assessed discrete anatomical features using in vitro  
54 data [2-13]. Being able to comprehensively characterise thoracic vertebral shape in vivo is  
55 essential for further research to improve our understanding of how spinal deformity initiates  
56 and progresses and for determining information that can be used to improve surgical  
57 techniques such as the placement of pedicle screws.

58 In vivo measurements of vertebral shape can be achieved using medical imaging data. A few  
59 studies have assessed thoracic vertebral shape in vivo using radiographs [14] or CT data [10,  
60 15]. These imaging modalities, however, incur a dose of ionising radiation and may not be  
61 suitable for all research studies, particularly longitudinal studies involving children or healthy  
62 control groups. Magnetic resonance image (MRI) data is an attractive alternative that avoids  
63 the use of ionising radiation, but the feasibility of using this imaging modality to reliably assess  
64 vertebral shape has not been established.

65 The shape of the vertebrae can be characterised using a number of different methods. Previous  
66 studies have tended to characterise shape by measuring individual dimensions and angles [2, 4,  
67 16]. This approach, however, makes it difficult to establish relationships between anatomical  
68 features and to separate variation in shape from variation in size. Shape modelling, which uses

69 statistical data analysis methods, provides a way of comprehensively characterising complex  
70 shapes, independently of size, using a small number of variables (modes of variation) where  
71 features that co-vary are included in the same mode of variation [17, 18]. Shape modelling has  
72 been used in a number of studies related to the spine [7, 19-22], and shown to be reliable [19],  
73 precise [19] and accurate [23], but has not been applied to characterising thoracic vertebrae.  
74 In this feasibility study, the primary aim was therefore to assess the reliability of characterising  
75 thoracic vertebral shape from MRI data using a shape model. The secondary aim was to  
76 estimate the amount of variation in thoracic vertebral shape in healthy volunteers and identify  
77 the factors that contribute to the variability.

## 78 **Material and Methods**

### 79 **Participants**

80 Twenty adult participants were recruited; the participants (12 female and 8 male) were aged 20  
81 to 53 years (median = 28 years). Ethical approval for the study was given by an ethics  
82 committee and written informed consent was obtained from all participants. Exclusion criteria  
83 were known deformity, arthritis, low bone density, previous injury, or surgery to the thoracic  
84 spine.

### 85 **Imaging**

86 Images of the participants' thoracic vertebrae were acquired using a 1.5 T Magnetic Resonance  
87 scanner (Intera, Philips, Amsterdam, The Netherlands) with a receive-only spine coil (Synergy,  
88 Philips, Amsterdam, The Netherlands). A T1-weighted turbo spin echo sequence was used  
89 (repetition time = 295 ms; echo time = 8 ms; number of signal averages = 3) that produced

90 images with an in-plane pixel size of 0.5 mm x 0.5 mm, a slice thickness of 1.9 mm and slice gap  
91 of 1.63 mm. A stack of 27 slices was acquired at each vertebral level, orientated parallel to the  
92 mid-transverse plane of the vertebral body. During scanning the participants were positioned  
93 supine. Each vertebral scan took just under 2.5 minutes and the time taken to set-up and  
94 complete scanning of the twelve vertebrae was approximately 40 minutes. After scanning, the  
95 participants were removed from the scanner, allowed to stretch and walk around for a few  
96 minutes, and then repositioned. Repeat scanning was performed at the levels of T4, T8 and  
97 T12; in four cases the repeat scan was performed one level below or above. Full data was  
98 collected for most participants (296 out of 300 datasets); the four missing datasets were due to  
99 scan errors.

#### 100 **Image annotation**

101 Each stack of 27 slices was visually inspected to find the slices that most clearly visualised the  
102 inferior facets, the spinous process, the pedicles, the vertebral body, the transverse processes,  
103 and the superior facets. This resulted in three to six slices being selected for each vertebra.  
104 These slices were then annotated by one observer (SJH) who manually placed landmark points  
105 using custom-written software tools in MATLAB [24]. The locations of the landmark points  
106 (Figure 1) were chosen to capture the anatomical features of the vertebral body and canal, the  
107 pedicles, the transverse and spinous processes, and the inferior and superior facets. A total of  
108 77 landmark points were used for each vertebra.

109 **Shape model**

110 The landmark points were used to create a shape model using software tools written in  
111 MATLAB [24]. The 296 sets of landmark points were aligned into a common reference frame  
112 using Procrustes analysis; this removed differences in the location, orientation and size of the  
113 vertebrae. The mean shape was determined and principle component analysis performed to  
114 identify modes of variation. The number of modes retained for analysis was determined using  
115 the broken-stick method which retains the modes that account for more variance than would  
116 be expected from a random model [25].  
117 Scores were given to each vertebra to describe its shape in terms of the retained modes of  
118 variation. The mean score, averaged across the 20 participants, at each vertebral level was then  
119 used to reconstruct the shape of the vertebrae at that level,  $Shape(T)$ , using equation 1.

120  $Shape(T) = Shape(mean) + \sum_{m=1}^N S(T, m)Shape(m)$  Equation 1

121 where  $Shape(mean)$  is the overall mean shape,

122  $S(T, m)$  is the mean score for mode  $m$  at vertebral level  $T$ ,

123  $Shape(m)$  is the shape described by mode  $m$ .

124 and  $N$  is the number of retained modes.

125 **Statistical analysis**

126 Statistical analysis was performed using SPSS [26] and a probability of 0.05 or less was taken to  
127 indicate statistical significance. The reliability of the mode scores was determined using the  
128 repeat data for T4, T8 and T12 (where a lower or higher level had been imaged it was matched



129 to its corresponding level in the initial data). Reliability was assessed using one-way analysis of  
130 variation to calculate the within-subject standard deviation of the repeated results. The three  
131 vertebral levels were treated separately to assess whether reliability varied along the spine and  
132 then pooled together to obtain an overall measurement error. The relative error was  
133 determined by multiplying the overall within subject standard deviation by 2.77 and expressing  
134 it as a percentage of the full range of values for the mode of variation being considered. Single  
135 measures intra-class correlation coefficients (ICC) were determined for the overall data using a  
136 one-way random model. ICCs were classed as being poor ( $0 < \text{ICC} < 0.4$ ), fair ( $0.4 < \text{ICC} < 0.59$ ), good  
137 ( $0.60 < \text{ICC} < 0.74$ ), or excellent ( $0.75 < \text{ICC} < 1$ ) [27].

138 The variability in the thoracic vertebrae shape and the effect of vertebral level, sex and age was  
139 assessed using repeated measures analysis of variance (full model with vertebral level as a  
140 within-subject factor, sex as a between-subject factor, and age as a covariate). The assumptions  
141 of sphericity were tested using Mauchly's sphericity test and, where these assumptions were  
142 violated, the Greenhouse-Geisser correction was used. Main effects were compared with a  
143 Sidak adjustment for multiple comparisons. Missing data for T1 from one participant was  
144 replaced by the mean of the other 19 participants so that this participant's data could be  
145 included in the repeated measures analysis of variance.

## 146 **Results**

### 147 **Modes of variation**

148 Five modes of variation (Figure 2) were retained from the shape model and accounted for 73 %  
149 of the total variance. Individually the modes accounted for 44 % (Mode 1), 19 % (Mode 2), 4 %

150 (Mode 3), 3 % (Mode 4), and 3 % (Mode 5) of the total variance. Visual inspection indicated that  
151 the first mode related to variation in the size of the vertebral bodies, the width and orientation  
152 of the pedicles, and the position and orientation of the processes and facet points. The second  
153 mode related to the size of the transverse processes and the ratio of the anteroposterior to  
154 lateral vertebral body diameter. The third mode related to the variation in the articular and  
155 costal facets and the relative size of the vertebral canal. The fourth mode related to curvature of  
156 the transverse processes and articular facets. The fifth mode related to variation in the location  
157 of the inferior and superior facets.

#### 158 **Reliability**

159 The reliability of the mode scores increased slightly from T4 to T12 (Table 1) but the increase  
160 was small and the overlap of the 95 % confidence intervals (with the exception of those of T4  
161 and T8 for mode 4) indicated that it was not significant. The overall error was therefore taken  
162 as representative for all vertebrae. The relative error and intra-class correlations showed that  
163 whilst modes 1 and 2 had excellent reliability, modes 3, 4 and 5 ranged from fair to good with a  
164 relative error up to 20 % of the data range.

#### 165 **Vertebral shape**

166 The mean mode scores (averaged across the 20 participants) demonstrated systematic trends  
167 along the thoracic spine (Figure 3) with scores decreasing monotonically from T1 to T12 for  
168 mode 1 and displaying a U-shaped variation for mode 2. For modes 3, 4 and 5 there was a less  
169 clearly defined pattern to the variation along the spine. The reconstructed vertebral shapes  
170 (Figure 4) reflect the variation demonstrated in Figure 3 with, for example, T1 having a high

171 score for both modes 1 and 2 that corresponds to a low anteroposterior to lateral diameter  
172 ratio and long transverse processes.

173 There was a significant effect of vertebral level on modes 1, 2 and 5 (Table 2). Pairwise  
174 comparisons (Figure 5) indicated that mode 1 differed significantly between nearly all pairs of  
175 vertebral levels and mode 2 differed significantly between most pairs of vertebrae except  
176 adjacent vertebrae in the middle of the spine and those at opposite ends of the spine. For  
177 mode 5 there were few significant differences between vertebral levels. The differences in the  
178 mode scores between male and female vertebrae were small (Figure 3) and the only significant  
179 for mode 3 (Table 2). There were no significant effects of age (Table 2).

## 180 **Discussion**

181 The primary aim of this study was to assess the reliability of using a shape model to  
182 characterise thoracic vertebral shape from MRI data acquired in vivo. Shape modelling is data  
183 analysis technique that is increasingly used to characterise the complex shape of anatomy. A  
184 particular advantage of shape modelling, over methods that involve making separate  
185 measurements of every individual anatomical feature of interest, is that it combines all  
186 correlated features into independent modes of variation. This makes the description of shape  
187 very efficient (using a small number of variables) and makes it easier to evaluate changes in  
188 shape due to the presence or progression of pathology. A recent example of this is the  
189 identification of changes in hip shape that may be related to the pathogenesis of hip  
190 osteoarthritis [28].

191 Shape modelling may be performed to characterise the three or two dimensional shape of  
192 anatomy. In our study, although 3D data was acquired, it was analysed as if it were projected  
193 2D data in the plane parallel to the mid-transverse plane of the vertebral body. This was done  
194 because a full 3D analysis would involve more landmark points and would require a larger  
195 sample of participants. The manual placement of landmark points can be time-consuming for  
196 large scale studies; however, methods of automatic landmark placement have been developed  
197 for studies using CT data [29] and progress is being made in being able to do the same using  
198 MRI data [30].

199 Our results show the use of a shape model on MRI data to be reliable with low relative error  
200 and high intra-class correlation. In this study repeated measurements were taken from two sets  
201 of image data, the second of which was acquired after repositioning the participant. This was  
202 done to simulate data acquired at multiple time-points, which would be the case in a  
203 longitudinal study that aimed to assess changes in vertebral shape over time. All the images  
204 were processed once by one observer which means that we cannot determine whether the  
205 main source of the error in our results of vertebral shape is the observer error in placing  
206 landmark points on the images or whether it is due to the images being slightly different after  
207 repositioning. Our previous work on the intra-observer and inter-observer reliability of placing  
208 landmark points on a single set of images, however, has found ICCs over 0.98 for the first two  
209 shape modes [19, 23] suggesting that repositioning did not have a great effect.

210 This study has also demonstrated, for the first time, the feasibility of using MRI data to  
211 characterise vertebral shape in vivo. A major advantage of MRI, over imaging modalities such as

212 CT, is the lack of ionising radiation. This makes it preferable, from a safety point of view, for use  
213 in healthy volunteers and also for repeated measurements in longitudinal studies, particularly  
214 those involving children who are particularly vulnerable to the effects of ionising radiation. MRI  
215 has not previously been used to characterise vertebral shape and this may stem from concerns  
216 that MRI data does not have sufficient quality for this type of study. Improvements in MRI  
217 technology over recent years, however, mean that image resolution can be as good as or even  
218 better than other modalities such as CT and issues such as low contrast between the bone and  
219 the surrounding tissue can be mitigated through the use of imaging sequences that enhance  
220 the contrast (although in our study we used standard T1-weighted imaging sequences and still  
221 achieved high reliability in our measurements). Finally, although MRI data can suffer from  
222 geometric distortion due to inhomogeneity in the MRI field gradients, this is predominantly a  
223 problem for data acquired using gradient-echo sequences. If non-gradient echo sequences are  
224 used (in our study we used spin-echo sequences) then it is likely that the data has a geometrical  
225 accuracy close to that of CT [31]. Other studies on the accuracy of using MRI data for  
226 determining bony anatomy in bones other than vertebrae have also concluded that it is  
227 comparable to CT [32, 33].

228 The secondary aim of our study was to estimate the variation in thoracic vertebral shape in  
229 healthy volunteers and identify the factors that contribute to the variability. The shape of the  
230 vertebra, and the variation in this shape along the thoracic spine, was found to be consistent  
231 with anatomical measurements reported in the literature. These include the anteroposterior  
232 diameter of the vertebral body increasing from T1 to T12 [4, 5]; the lateral diameter of the  
233 vertebral body decreasing from T1 to T3 or T4 followed by an increase to T12 [5]; the lateral

234 width of the vertebral canal decreasing from T1 to T5 followed by an increase to T12 [4, 13]; the  
235 pedicle width decreasing from T1 to T4 followed by little variation until T8 where it increases to  
236 T12 [8-11]; the pedicle angle decreasing from T1 to T12 [8, 9]; the transverse process changing  
237 from a more lateral orientation at T1 to a more posterior orientation T12 [12, 15]; and the  
238 length of transverse processes increasing slightly from T1 to the mid-thoracic region and then  
239 decreasing towards T12 [12]. The effect of vertebral level on the shape was found to be  
240 significant.

241 The shape of the vertebrae was very similar in males and females and although there were  
242 differences in the scores for modes 3 and 4, only mode 3 reached statistical significance.  
243 Nevertheless, the differences in these modes describe variation in shape that is consistent with  
244 results that have found the transverse processes to be more dorsally orientated, and the neural  
245 canal to be smaller, in males compared to females [7]. Previous studies that have identified  
246 large differences between male and female vertebrae have assessed absolute measurements  
247 but these reflect the larger size of the male vertebrae [4] which was not considered in the  
248 current study due to scale being removed from the model. Age was not found to have a  
249 relationship with vertebral shape in. A previous study has found changes in the relative  
250 dimensions of the thoracic vertebrae with age [34] but these were based on measurements in  
251 the sagittal plane which were not considered in the current study.

252 Our study has demonstrated that the shape of the thoracic vertebra can be characterised  
253 comprehensively and reliability from MR data using a statistical shape model. This suggests that  
254 the methods would be useful for future longitudinal studies; however, as our sample comprised

255 twenty healthy volunteers, subsequent studies should independently repeat the assessment of  
256 reliability since our values, particularly those of the ICC which depend on sample heterogeneity,  
257 are unlikely to be generalizable to all samples. The correspondence between the results of our  
258 study and measurements reported in the literature demonstrates that the shape model is able  
259 to correctly characterise known variation in vertebral shape along the thoracic spine. This  
260 suggests that the technique may be powerful enough to detect differences between normal  
261 and pathological vertebrae. The differences found between male and female, although small,  
262 suggest it is important to conduct future studies on single sexes or include sex as an additional  
263 factor.

264 **References**

- 265 1. Abul-Kasim K, Ohlin A. Patients with adolescent idiopathic scoliosis of Lenke type-1 curve exhibit  
266 specific pedicle width pattern. *Eur Spine J* 2012;21:57-63.
- 267 2. Berry JL, Moran JM, Berg WS et al. A morphometric study of human lumbar and selected thoracic  
268 vertebrae. *Spine* 1987;12:362-7.
- 269 3. Hou S, Hu R, Shi Y. Pedicle morphology of the lower thoracic and lumbar spine in a Chinese  
270 population. *Spine* 1993;18:1850-5.
- 271 4. Masharawi Y, Salame K. Shape variation of the neural arch in the thoracic and lumbar spine:  
272 Characterization and relationship with the vertebral body shape. *Clin Anat* 2011;24:858-67.
- 273 5. Masharawi Y, Salame K, Mirovsky Y et al. Vertebral body shape variation in the thoracic and lumbar  
274 spine: Characterization of its asymmetry and wedging. *Clin Anat* 2008;21:46-54.
- 275 6. Chung KJ, Suh SW, Desai S et al. Ideal entry point for the thoracic pedicle screw during the free hand  
276 technique. *Int Orthop* 2008;32:657-62.
- 277 7. Bastir M, Higuero A, Rios L et al. Three-dimensional analysis of sexual dimorphism in human thoracic  
278 vertebrae: implications for the respiratory system and spine morphology. *Am J Phys Anthropol*  
279 2014;155:513-21.
- 280 8. Cinotti G, Gumina S, Ripani M et al. Pedicle instrumentation in the thoracic spine: a morphometric and  
281 cadaveric study for placement of screws. *Spine* 1999;24:114-9.
- 282 9. Parent S, Labelle H, Skalli W et al. Thoracic pedicle morphometry in vertebrae from scoliotic spines.  
283 *Spine* 2004;29:239-48.
- 284 10. Pai BS, Nirmala S, Muralimohan S et al. Morphometric analysis of the thoracic pedicle: an anatomico-  
285 radiological study. *Neurol India* 2010;58:253-8.



- 286 11. Morales-Avalos R, Leyva-Villegas J, Sanchez-Mejorada G et al. Age- and gender-related variations in  
287 morphometric characteristics of thoracic spine pedicle: A study of 4,800 pedicles. *Clin Anat* 2014;27:441-  
288 50.
- 289 12. Cui XG, Cai JF, Sun JM et al. Morphology study of thoracic transverse processes and its significance in  
290 pedicle-rib unit screw fixation. *J Spinal Disord Tech* 2015;28:E74-7.
- 291 13. Cho SK, Skovrlj B, Lu Y et al. The effect of increasing pedicle screw size on thoracic spinal canal  
292 dimensions: an anatomic study. *Spine* 2014;39:E1195-E200.
- 293 14. Zindrick MR, Wiltse LL, Doornik A et al. Analysis of the morphometric characteristics of the thoracic  
294 and lumbar pedicles. *Spine* 1987;12:160-6.
- 295 15. Zhuang Z, Xie Z, Ding S et al. Evaluation of thoracic pedicle morphometry in a Chinese population  
296 using 3D reformatted CT. *Clin Anat* 2012;25:461-7.
- 297 16. Ebraheim NA, Xu R, Ahmad M et al. Projection of the Thoracic Pedicle and Its Morphometric  
298 Analysis. *Spine* 1997;22:233-8.
- 299 17. Cootes TF, Taylor CJ. Anatomical statistical models and their role in feature extraction. *Br J Radiol*  
300 2004;77:S133-S9.
- 301 18. Heimann T, Meinzer H-P. Statistical shape models for 3D medical image segmentation: a review.  
302 *Med Image Anal* 2009;13:543-63.
- 303 19. Meakin JR, Gregory JS, Smith FW et al. Characterizing the shape of the lumbar spine using an active  
304 shape model: reliability and precision of the method. *Spine* 2008;33:807-13.
- 305 20. Meakin JR, Smith FW, Gilbert FJ et al. The effect of axial load on the sagittal plane curvature of the  
306 upright human spine in vivo. *J Biomech* 2008;41:2850-4.
- 307 21. Meakin JR, Gregory JS, Aspden RM et al. The intrinsic shape of the human lumbar spine in the  
308 supine, standing and sitting postures: characterization using an active shape model. *J Anat*  
309 2009;215:206-11.

- 310 22. Peloquin JM, Yoder JH, Jacobs NT et al. Human L3L4 intervertebral disc mean 3D shape, modes of  
311 variation, and their relationship to degeneration. *J Biomech* 2014;47:2452-9.
- 312 23. Ali A, Cowan A-b, Gregory J et al. The accuracy of active shape modelling and end-plate  
313 measurements for characterising the shape of the lumbar spine in the sagittal plane. *Comput Methods*  
314 *Biomech Biomed Engin* 2012;15:167-72.
- 315 24. MATLAB [Computer Program]. Version R2017a. Natick, Massachusetts: The MathWorks Inc., 2017.
- 316 25. Jackson DA. Stopping rules in principal components analysis: a comparison of heuristical and  
317 statistical approaches. *Ecology* 1993;74:2204-14.
- 318 26. IBM SPSS Statistics for Windows [Computer Program]. Version 23. Armonk, New York: IBM Corp.,  
319 2015.
- 320 27. Cicchetti DV. Guidelines, criteria, and rules of thumb for evaluating normed and standardized  
321 assessment instruments in psychology. *Psychol Assess* 1994;6:284-90.
- 322 28. Faber BG, Baird D, Gregson CL et al. DXA-derived hip shape is related to osteoarthritis: findings from  
323 in the MrOS cohort. *Osteoarthritis Cartilage* 2017;25:2031-8.
- 324 29. Campbell JQ, Petrella AJ. An automated method for landmark identification and finite-element  
325 modeling of the lumbar spine. *IEEE Trans Biomed Eng* 2015;62:2709-16.
- 326 30. Hutt H. *Automatic segmentation of the lumbar spine from medical images* [PhD Thesis]: University of  
327 Exeter; 2016.
- 328 31. Rathnayaka K, Momot KI, Noser H et al. Quantification of the accuracy of MRI generated 3D models  
329 of long bones compared to CT generated 3D models. *Med Eng Phys* 2012;34:357-63.
- 330 32. Van den Broeck J, Vereecke E, Wirix-Speetjens R et al. Segmentation accuracy of long bones. *Med*  
331 *Eng Phys* 2014;36:949-53.
- 332 33. van Eijnatten M, Rijkhorst E-J, Hofman M et al. The accuracy of ultrashort echo time MRI sequences  
333 for medical additive manufacturing. *Dentomaxillofac Radiol* 2016;45:20150424.

334 34. Goh S, Tan C, Price RI et al. Influence of age and gender on thoracic vertebral body shape and disc  
335 degeneration: an MR investigation of 169 cases. *J Anat* 2000;197:647-57.

336

337

338 Table 1. Reliability of the mode scores. The within-subject standard deviation (95 % confidence interval) is shown individually for the  
 339 three vertebral levels and overall. The relative error indicates the measurement error as a percentage of the range.

<b>Mode</b>	<b>T4</b>	<b>T8</b>	<b>T12</b>	<b>Overall</b>	<b>Relative overall</b>	<b>ICC</b>
<b>1</b>	0.11 (0.07 - 0.15)	0.13 (0.08 - 0.17)	0.16 (0.1 - 0.21)	0.13 (0.11 - 0.16)	7%	0.98 (0.97 - 0.99)
<b>2</b>	0.15 (0.10 - 0.20)	0.17 (0.12 - 0.23)	0.24 (0.16 - 0.32)	0.19 (0.15 - 0.22)	11%	0.96 (0.94 - 0.98)
<b>3</b>	0.49 (0.32 - 0.65)	0.51 (0.34 - 0.68)	0.73 (0.48 - 0.99)	0.58 (0.47 - 0.69)	27%	0.70 (0.54 - 0.81)
<b>4</b>	0.32 (0.21 - 0.42)	0.71 (0.47 - 0.94)	0.72 (0.47 - 0.97)	0.61 (0.50 - 0.72)	21%	0.57 (0.37 - 0.73)
<b>5</b>	0.59 (0.39 - 0.80)	0.42 (0.28 - 0.56)	0.40 (0.26 - 0.54)	0.48 (0.39 - 0.57)	16%	0.68 (0.52 - 0.80)

340

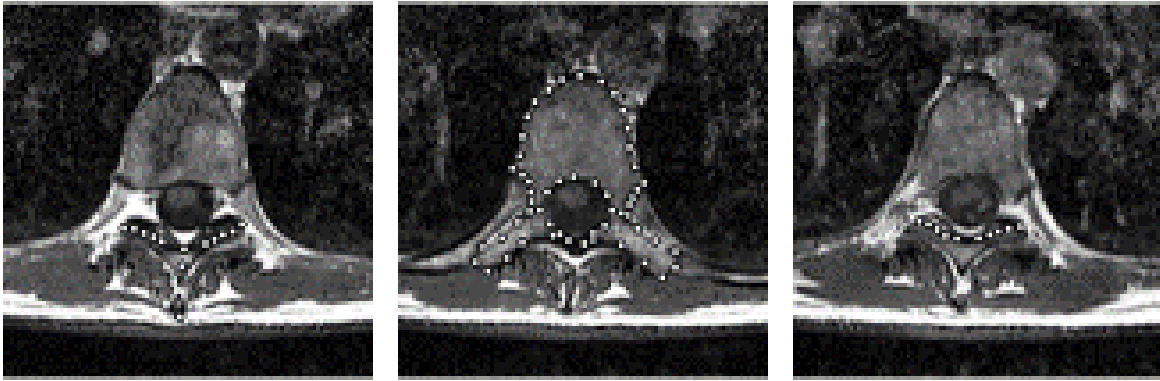
341

342 Table 2. The effect of vertebral level, sex and age on the mode scores, assessed using repeated  
343 measures analysis of variance.

	<b>Vertebral level</b>		<b>Sex</b>		<b>Age</b>	
	F-statistic	P value	F-statistic	P value	F-statistic	P value
<b>Mode 1</b>	23	< 0.001	1.0	0.34	2.7	0.12
<b>Mode 2</b>	14	< 0.001	0.7	0.40	0.1	0.77
<b>Mode 3</b>	1.0	0.41	7.7	0.01	0.02	0.89
<b>Mode 4</b>	1.8	0.11	3.2	0.09	0.1	0.76
<b>Mode 5</b>	2.6	0.03	0.03	0.87	3.4	0.08

344

345

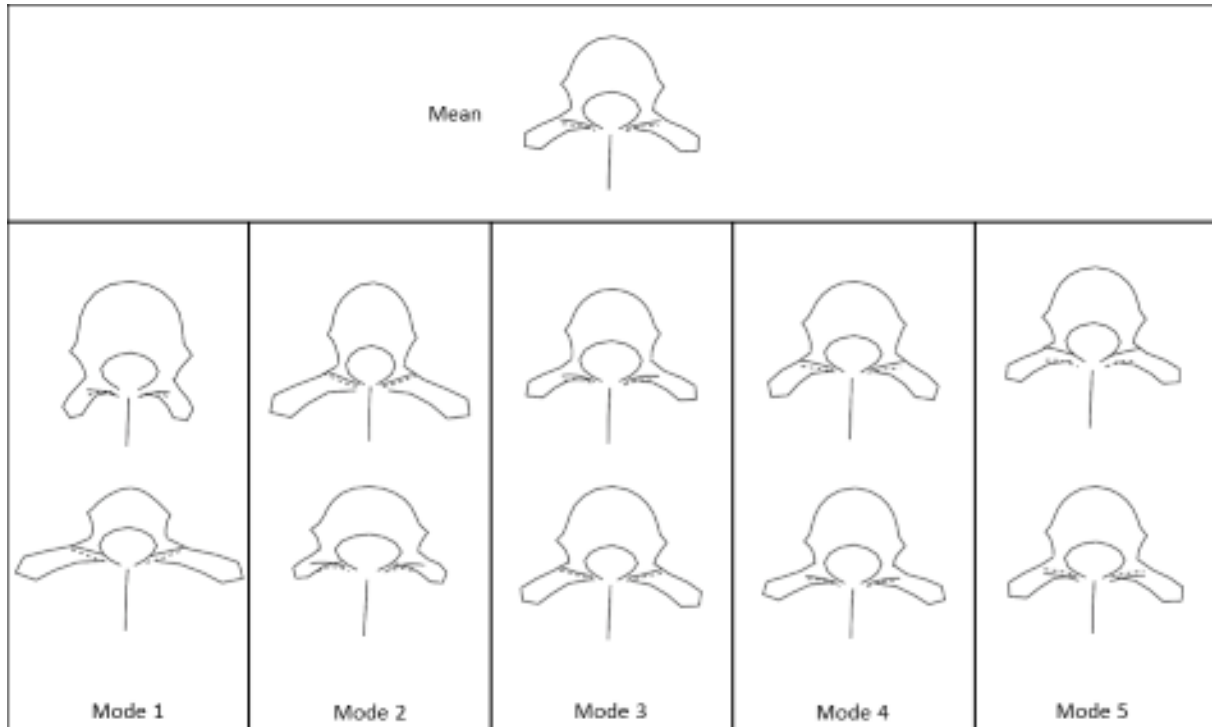


346

347 Figure 1. Three slices from a vertebra stack showing the placement of the 77 landmark points.

348

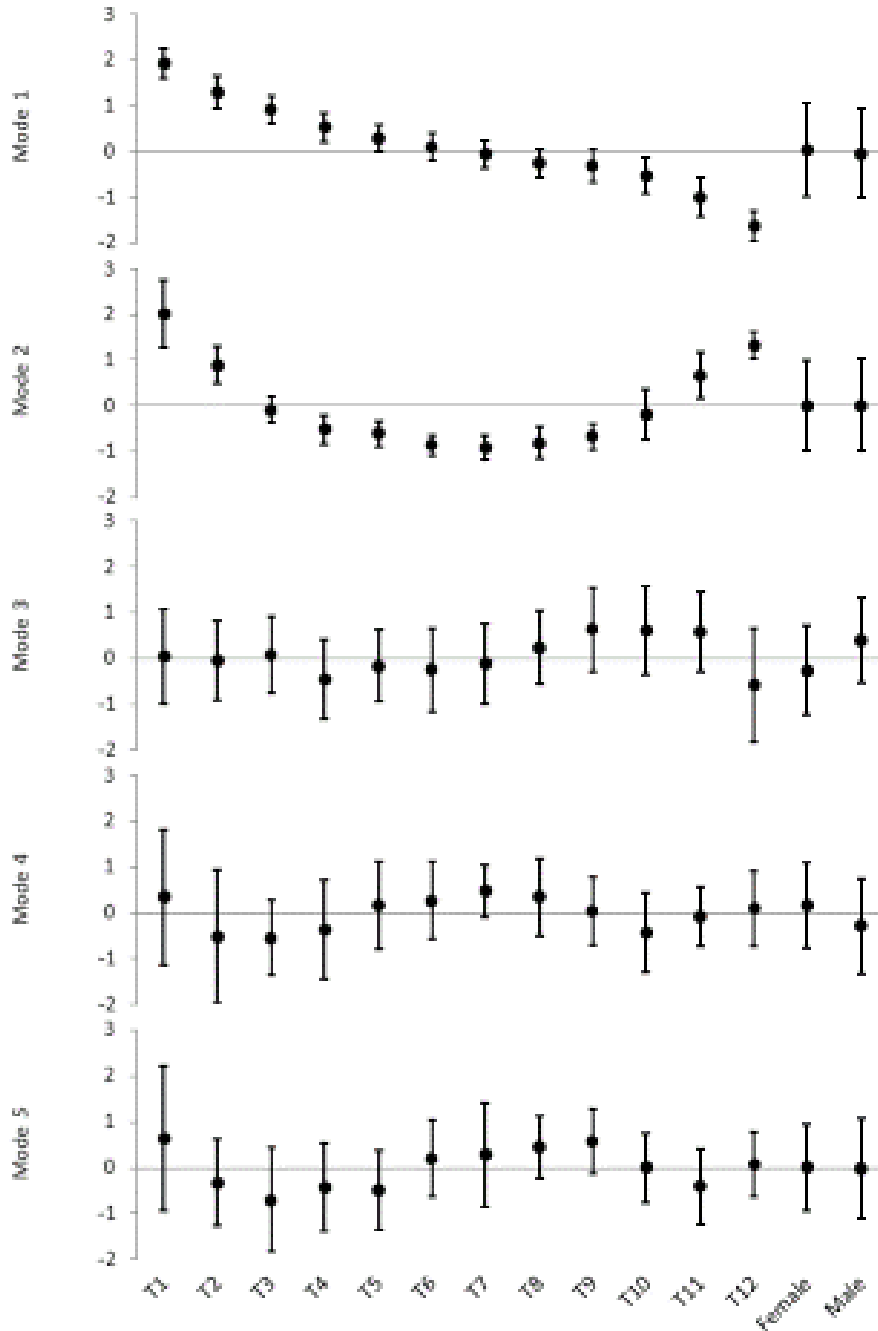
349



350

351 Figure 2. Mean shape and first five modes of variation. For each mode the upper image shows  
 352 +2 standard deviations, and the lower image -2 standard deviations, from the mean shape. The  
 353 superior facet is shown as a solid line and the inferior facet as a dashed line.

354



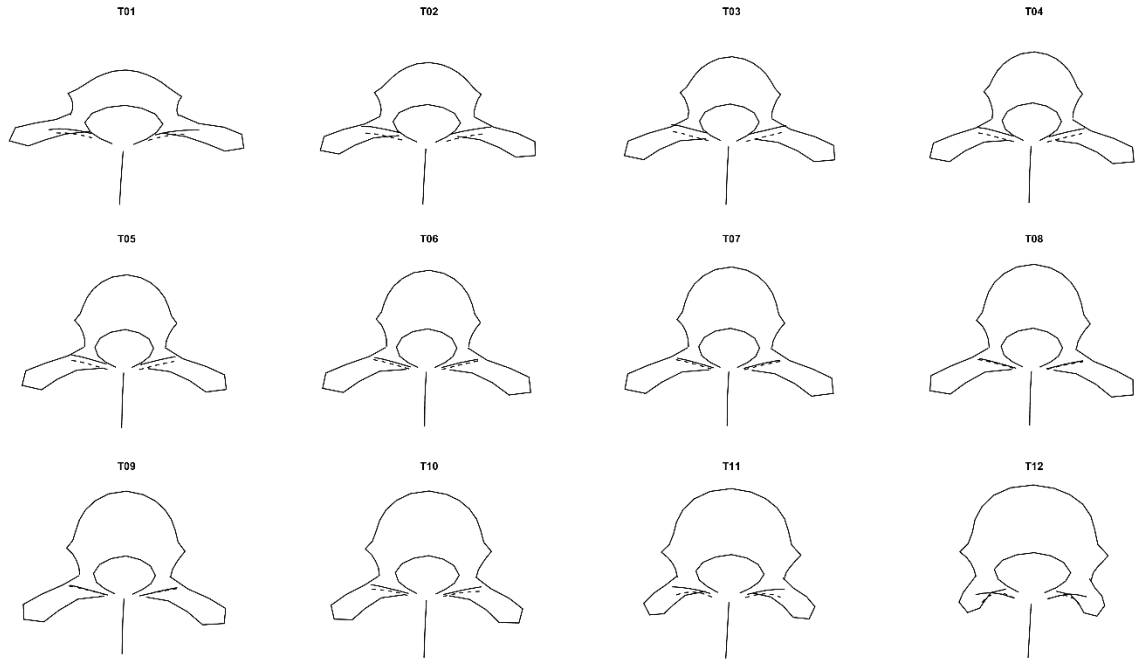
355

356 Figure 3. Mode scores along the thoracic spine (T1-T12) and for males and females. Data points

357 indicate the mean values (n = 20 (T1-T12), 8 (male), 12 (female)) with error bars showing 1

358 standard deviation.





359

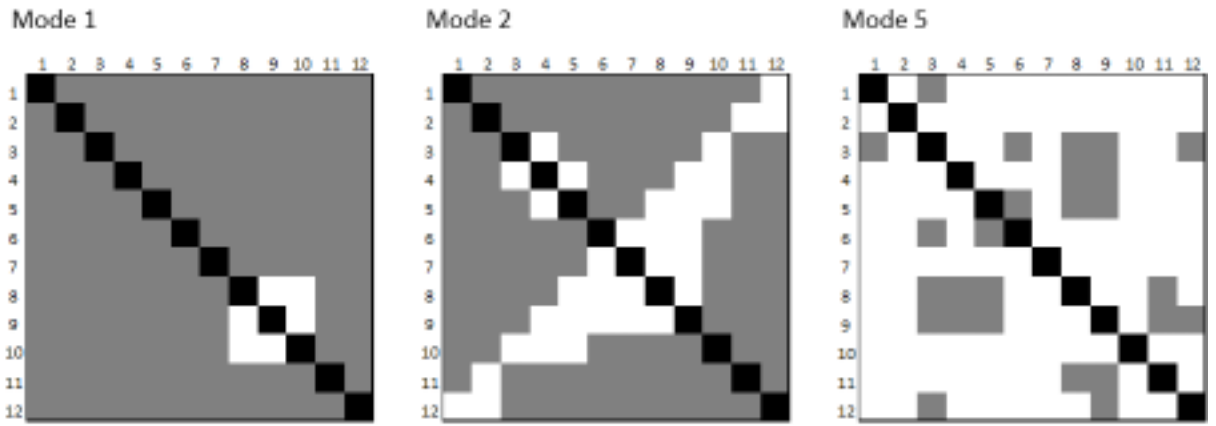
360

361

362

363

Figure 4. Mean thoracic vertebral shape. The shape of each vertebra represents the mean of the 20 participants and was reconstructed from the first 5 modes. The superior facet is shown as a solid line and the inferior facet as a dashed line.



364

365 Figure 5. Visualisation of the results of the pairwise comparisons between vertebrae mode  
 366 scores. Grey: significantly different ( $p < 0.05$ ), white: not significantly different ( $p > 0.05$ ), black:  
 367 not applicable.